# Numerical and experimental comparison of 3D-model for the study of railway vibrations

Benoit Picoux, Donatien Le Houédec

# Numerical and Experimental Comparison of 3D-Model for the Study of Railway Vibrations

**B. Picoux† and D. Le Houédec‡**
**†Institut Universitaire de Technologie**
**Département Génie Civil, Saint-Nazaire, France**
**‡Ecole Centrale de Nantes, Laboratoire Mécanique et Matériaux, Nantes, France**

## Abstract

This paper describes a 3D-model developed for the prediction of vibrations near a railway track [3]. It consists of a track model lying on a layered ground and submitted to a moving train. It includes all elements of the track (rails, pads, sleepers and ballast) [5] and allows a parametric analysis of its different elements and evaluation of vertical displacements according to the speed, the weight and the composition of the trains. Then *in situ* measurements are introduced with a view to the validation of the numerical model. A parameter study of the ground undertaken by seismic measurements shows a critical speed near 100 m/s while the studied trains are moving with sub-Rayleigh speeds (20 to 50 m/s). Consequently, all the parameters needed for the numerical model are defined. Many measurements were performed with a fast numerical camera which allows to notice the sheer size of the stress subjected to the track. Synchronised measurements of soil surface acceleration and track elements velocity were recorded. They give us a lot of informations about lateral and vertical displacements of track elements and at the soil surface. For highest speeds and freight trains, measured displacements reach more than about 10 millimetres.

Finally, results are validated for different configurations. Measurements and simulation are compared in the time domain and in the term of spectral density. A comparison against distance of the track is also done and shows that contribution of the harmonic regime due to irregularities becomes more important farther from the track. The great agreement found in the validation confirmed the good quality of the determination of mechanical parameters, particularly the parameters which depend on compression and shear waves speed.

**Keywords:** wave propagation, railway track, moving loads (train), Fourier transform, soft soils, *in situ* measurements.

# 1 Introduction

In the North West of Europe, more particularly in the region of the Somme Bay in France where grounds are mainly constituted by saturated peat, observations and measurements have revealed the presence of great displacements at the soil surface near railway tracks and in the track itself. In very soft soil conditions composing of a low Young modulus and important water content, these displacements can cause not only harmful effects for the neighbourhood of the track and the surrounding buildings but also damage or fracture in the track. These pollutions also depend on the weight and the speed of the train mainly when this speed is close to a critical speed corresponding to the Rayleigh wave speed [4].

Track models have been studied by many authors and used different formulations. Krylov [3] introduced a model based on the use of Green functions, Degrande & Lombert [1] used a finite elements method. Many authors have used the Fourier transform considering the sleeper spacing (Metrikine & Popp [6]) or supposing perfect homogeneity and track continuity (Sheng & Jones [8]).

Our model is built according to this principle and especially for low frequencies. The studied soil is supposed to be homogeneous and isotropic in each layer. It is composed by a ballast layer and a thick peat layer. A rigid halfspace extends beneath this soft layer. The railway track is composed by a rail lying on wood sleepers joined by pads. Railway excitation is modelled like a real train with simplified but multi-frequential harmonic excitation. On the whole study, comparison between 3D-model and *in situ* measurements leads to good results taking into account measurements difficulties, important number of unknown parameters and hypothesis of linearity of track elements and homogeneity of soil layers. Particular velocities and maximum displacements at 2 and 5 meters from the track were compared to simulation results.

In a first part, the three dimensional model of track soil interaction will be introduced. Then , main results of experimental part will be detailed and finally the validation of the model will be able to be done.

# 2 Three - Dimensional model of track-soil interaction

The mathematical model of track performed in a code named FASTIVIB is obtained with few simplifications :

- Each rail is considered like a perfectly elastic Euler beam,
- Each sleeper is modelled like a sum (continue) of stiffness elements offering a lateral and longitudinal resistance,
- Pads are considered like continuum elements having stiffness and damping between rail and sleepers,
- Ballast is easily constituted by an elastic layer lying on soil.

## 2.1 Mathematical model

The resolution method uses the formalism of Fourier transform for a semi-analytical resolution in the wave number domain [1]. The handwriting of a stiffness matrix for a layered ground with the help of a fitted phase angle of Helmoltz functions provides a fast numerical approach of the problem. Equations are written in the wave numbers domain and for steady state solutions. A numerical inverse Fourier transform is applied when the matrix equation of the whole system (train - track - soil) has been resolved.

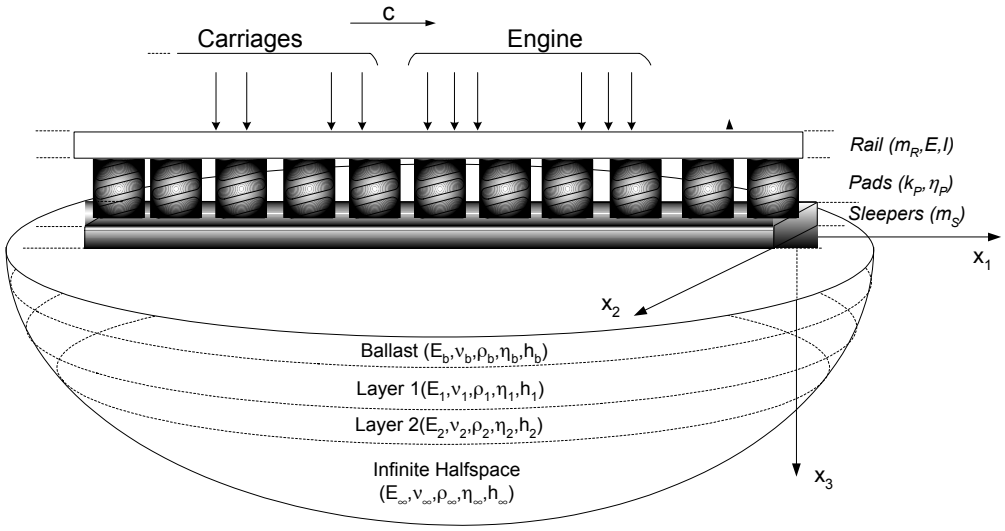


Figure 1: 3D-Model of soil-track interaction.

### 2.2.1 Semi-analytical model

The soil is homogeneous and isotropic. Intrinsic parameters for a ground layer are Young's modulus E, Poisson's ratio $\nu$, density $\rho$, hysteretic damping factor $\eta$ and thickness h. For a layered ground, a rigidity matrix connecting stresses with displacements at the interface of each layer can be written. However, convergence problems for some terms have been noticed needing to divide layers in sub-layers.

This problem is solved thanks to the notion of fitted phase argument in the Helmoltz potentials. This modification provides a well conditioned matrix and then a saving of computation time.

Then, Helmoltz potentials $\phi$ and $\psi$ are written as :

$$\begin{cases} \phi = Ae^{\alpha_1(z-h)} + Ce^{-\alpha_1 z} \\ \psi = Be^{\alpha_2(z-h)} + De^{-\alpha_2 z} \end{cases} \quad (1)$$

where $\alpha_i$ depends on wave numbers, train speed and excitation frequency.

In the absence of body forces, the combination of the equation of movement and the behaviour law gives the Navier equation :

$$(\lambda+\mu)u_{l,li}+\mu u_{i,ll}=\rho\frac{\partial^2 u_i}{\partial t^2} \qquad (2)$$

where $\lambda$ and $\mu$ are the Lamé's coefficients, i denotes the three co-ordinates and $u_i$ are linked to $\psi$ and $\phi$.
The damping law carried for the ground is hysteretic leading to a factor $(1+i\eta sign(\omega))$ in the Lamé's coefficient and in the Young's modulus where $\omega$ is the angular frequency of excitation.

For the case of a three-dimensional layered ground and by taking into account the fitted phase argument, the new dilatation function $\theta$ after a change of functions and change of variables [2] becomes in the wave number domain $(\beta,\gamma)$ :

$$\overline{\theta}^* = i\beta\overline{u}^* + i\gamma\overline{v}^* + \frac{d\overline{w}^*}{dz} = \overline{A}e^{\alpha_1(z-h)} + \overline{B}e^{-\alpha_1 z} \qquad (3)$$

Then the wave motion is written as :

$$\left(\frac{d^2}{dz^2}-\alpha_2^2\right)\begin{Bmatrix}\overline{u}^*\\ \overline{v}^*\\ \overline{w}^*\end{Bmatrix} = -\frac{\lambda+\mu}{\mu}\begin{Bmatrix} i\beta(\overline{A}e^{\alpha_1(z-h)}+\overline{B}e^{-\alpha_1 z})\\ i\gamma(\overline{A}e^{\alpha_1(z-h)}+\overline{B}e^{-\alpha_1 z})\\ \alpha_1(\overline{A}e^{\alpha_1(z-h)}-\overline{B}e^{-\alpha_1 z})\end{Bmatrix} \qquad (4)$$

The solution of this equation is given by the sum of a general solution of the equation without second member and a particular solution of the equation with second member, such as :

$$\begin{Bmatrix}\overline{u}^*\\ \overline{v}^*\\ \overline{w}^*\end{Bmatrix} = -\frac{\overline{A}e^{\alpha_1(z-h)}}{k_1^2\left(1-\frac{\beta c}{\omega}\right)^2}\begin{Bmatrix}-i\beta\\ -i\gamma\\ -\alpha_1\end{Bmatrix} + \frac{\overline{B}e^{\alpha_1(z-h)}}{k_1^2\left(1-\frac{\beta c}{\omega}\right)^2}\begin{Bmatrix}-i\beta\\ -i\gamma\\ \alpha_1\end{Bmatrix}$$
$$+ e^{\alpha_2(z-h)}\begin{Bmatrix}\overline{C}\\ \overline{D}\\ -\frac{i}{\alpha_2}(\beta\overline{C}+\gamma\overline{D})\end{Bmatrix} + e^{-\alpha_2 z}\begin{Bmatrix}\overline{E}\\ \overline{F}\\ \frac{i}{\alpha_2}(\beta\overline{E}+\gamma\overline{F})\end{Bmatrix} \qquad (5)$$

where $\overline{A}$, $\overline{B}$, $\overline{C}$, $\overline{D}$, $\overline{E}$ and $\overline{F}$ depend on the angular frequency $\omega$.

### 2.2.2 Matrix formulation

Displacements for a layer of thickness h can be written :

$$\left\{\overline{U}^*\right\}=\left\{\overline{u}_0^* \quad \overline{v}_0^* \quad i\overline{w}_0^* \quad \overline{u}_h^* \quad \overline{v}_h^* \quad i\overline{w}_h^*\right\}^T=[Q]\left\{\overline{A} \quad \overline{B} \quad \overline{C} \quad \overline{D} \quad \overline{E} \quad \overline{F}\right\}^T \qquad (6)$$

and the longitudinal, lateral and vertical stresses are written respectively such as :

$$\frac{\overline{\tau}_{xz}^*}{\mu}=\frac{d\overline{u}^*}{dz}+i\beta\overline{w}^* \;;\; \frac{\overline{\tau}_{yz}^*}{\mu}=\frac{d\overline{v}^*}{dz}+i\gamma\overline{w}^* \;;\; \frac{\overline{\sigma}_{zz}^*}{\mu}=\frac{\lambda}{\mu}\overline{\theta}^*+2\frac{d\overline{w}^*}{dz} \qquad (7)$$

Stresses for a layer of thickness h can be similarly written :

$$\left\{\overline{\Sigma}^*\right\}=\left\{-\overline{\tau}_{xz,0}^* \quad -\overline{\tau}_{yz,0}^* \quad -i\overline{\sigma}_{zz,0}^* \quad \overline{\tau}_{xz,h}^* \quad \overline{\tau}_{yz,h}^* \quad i\overline{\sigma}_{zz,h}^*\right\}^T=[S]\left\{\overline{A} \quad \overline{B} \quad \overline{C} \quad \overline{D} \quad \overline{E} \quad \overline{F}\right\}^T \qquad (8)$$

Finally, a stiffness matrix which connects displacements vector U with stresses vector Σ can be deduced :

$$[S]\times[Q]^{-1}\left\{\overline{U}^*\right\}=[R]\left\{\overline{U}^*\right\}=\left\{\overline{\Sigma}^*\right\} \qquad (9)$$

Inversion of [Q] and its multiplication by [S] give the rigidity matrix [R]. It is no longer necessary to divide each layer into sub-layers according to the convergence of each term. So a saving of calculation time has been performed.

For the entire model, the contribution of the ballast which is assumed to be the first layer is found in the upper left side of [R]. The contribution of the n soft layers and the contribution of the half-space (lower right) are also included. But the contributions of the rail, pads and sleepers are included in the stress vector. In the case of a vertical stress, the stress vector is reduced to a single component vector. This vector is given in the next part. The transformed displacements can be calculated analytically and then inverse Fourier transform gives the actual displacements. Analytical inverse Fourier transform with residual method can be performed for a semi infinite soil but numerical inverse Fourier transform is necessary for a layered ground. The final stiffness matrix is built from matrices [Q], [S] and [R] introduced in [7].

### 2.2.3 Railway track excitation

Considering the axis $(O,x_1, x_2,x_3)$ connected to the soil and (O',x,y,z) connected to the moving load, differential equation for the rail in $(O,x_1,x_3)$ (as Euler beam) can be written as :

$$EI\frac{\partial^4 w_R(x_1,t)}{\partial x_1^4}+m_R\frac{\partial^2 w_R(x_1,t)}{\partial t^2}+k_P\left[w_R(x_1,t)-w_S(x_1,t)\right]=\begin{cases}\dfrac{P_0 e^{i\Omega_0 t}}{2b} & \text{pour } |x_1-ct|<b \\ 0 & \text{sinon}\end{cases} \qquad (10)$$

where $x_1$ -ct means the displacement of the load.

A damping coefficient $\eta_R$ can also be added in rail equation as :

$$(EI)^* = (EI)(1+i\eta_R) \qquad \text{where} \qquad \eta_R = 0{,}04 \qquad (11)$$

Because of the few length of the sleeper spacing against the length of the rail deflexion at low frequency, a distributed mass representing sleepers is used in the track. Then, the sleeper equation is :

$$m_S \frac{\partial^2 w_S(x_1,t)}{\partial t^2} + k_P\left[w_S(x_1,t) - w_R(x_1,t)\right] = -F_S(x_1,t) \qquad (12)$$

where $F_S$ means force acting on a sleeper by rail.

Finally the ballast is constituted by an elastic layer laying on soil and included in stiffness soil matrix. Damping in pads and sleepers are taking into account with a damping coefficient $\eta_i$ in the stiffness like $k_i^*=k_i[1+i\eta_i sign(\omega)]$. Numerical values for all these parameters are given in table 1.

| Elements | Mechanical parameters |
|---|---|
| Rails | $E = 2.11\times10^{11}$ N.m$^{-2}$ ; $I = 3055$ cm$^4$ ; $m_R = 60.34$ kg.m$^{-1}$ |
| Pads | $\eta_P = 0.2$ ; $k_P = 60\times10^6$ N.m$^{-2}$ |
| Sleepers (Wood) | $m_S = 191$ kg.m$^{-1}$ |
| Ballast | $E_b = 300$ MPa ; $\nu_b = 0.3$ ; $\rho_b = 1800$ kg.m$^{-3}$ ; $\eta_b = 0.1$ |

Table 1 : Track parameters.

The railway train excitation is composed by vertical forces (see figure 1). It represents the effect of each wheel of the engine and carriages acting directly on the rail. Each of these forces is supposed to be equal to a harmonic excitation $P_0 e^{i\Omega_0 t}$. The total weight of the load is distributed on the rail - wheel contacts.

The Cauchy stress due to engine can be written as :

$$\bar{\sigma}_{ENG}(\beta) = -2P_{ENG} e^{i\Omega_0 t} e^{-i\frac{\beta}{2}(N_{CAR}L_{CAR}+L_{ENG})} \frac{\sin\beta a}{\beta a}\left[1+2\cos\beta L_{BOG-ENG}\right]\cos\beta L_{AX-ENG} \qquad (13)$$

and the Cauchy stress due to $2N_{CAR}$ carriages :

$$\bar{\sigma}_{CAR}(\beta) = -4P_{CAR} e^{i\Omega_0 t} \frac{\sin\beta a}{\beta a}\cos\beta L_{AX-ENG}\cos\beta L_{BOG-CAR} \sum_{k=1}^{2N_{CAR}} e^{i\beta\left(k-\frac{N_{CAR}}{2}-\frac{1}{2}\right)L_{CAR}} \qquad (14)$$

where $L_{BOG}$ means the distance of wheel spacing in boggie and $L_{AX}$ means the distance between two axles.

Finally $\bar{\sigma}_{TRAIN}(\beta) = \bar{\sigma}_{ENG}(\beta) + \bar{\sigma}_{WAG}(\beta)$.

The whole excitation is a frequency dependant function supposing to occur in a range 0-80Hz [6]. It includes a quasi-static component produced by the weight of all axle loads and a harmonic component generated by irregularity between rail and wheel. Static and quasi-static components are more important near the track. The model used for vibration comparisons at 2 metres or 3 metres from the track will be able to consider the contribution of static component and harmonic component at low frequency. A linear function of the frequency [0,40 Hz] or gaussian function can be used for the wheel excitation on the track.

## 2.2 Numerical results

First of all, a 10 Hz excitation frequency is chosen in the numerical model. Mechanical parameters are chosen for representing a test soil (one sand layer $E = 269$ MPa ; $\nu = 0{,}257$ ; $\rho = 1550$ kg.m$^{-3}$ ; $\eta = 0{,}1$ ; $h = 7$ m on infinite halfspace $E = 2040$ MPa ; $\nu = 0{,}179$ ; $\rho = 2450$ kg.m$^{-3}$ ; $\eta = 0{,}1$). Displacements field at soil surface is represented on figure 2 for speeds inferior to the Rayleigh wave speed ($0.5 \times c_R$) and superior to the Rayleigh wave speed ($1.5 \times c_R$).

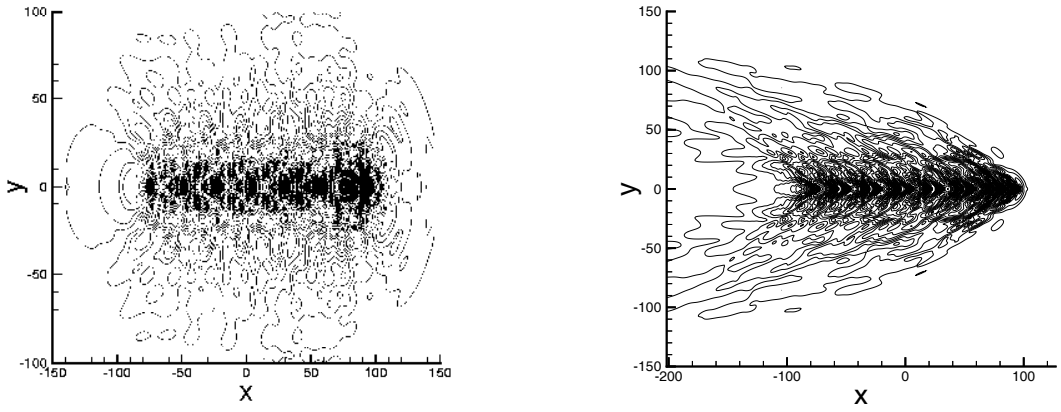


Figure 2 : Displacements field at soil surface for "Corail" train in sub-Rayleigh speed (left) and super-Rayleigh speed (right).

If the load speed is fewer than the phase velocity of the system, displacements produced by the single applied forces which composed the train are quickly reduced (evanescent wave). In this case, energy is confined in the vicinity of this load. Nevertheless, if the load speed is high enough to excite one of the propagation mode in the system then the response of the system increases because of each single load (constructive interference).

Figure 2 shows that increase of load speed implies a great amplification of vertical displacements and increase of oscillations behind the train. Displacements fields are plotted for different velocities of a "Corail" train (current French train : 1 engine and 6 carriages) and confirm previous results as well as the presence of Mach cones for each bogie load.

Now the soil is considered as a soft soil (peat layer : E = 68 MPa ; $\nu = 0{,}43$ ; $\rho = 1600$ kg.m$^{-3}$ ; $\eta = 0{,}05$ ; h = 7 m and limestone substratum : E = 3989 MPa ; $\nu = 0{,}35$ ; $\rho = 2000$ kg.m$^{-3}$ ; $\eta = 0{,}1$).

Figure 3 shows performed response of soil surface against the distance from the track and the aspect of quasi-static displacements near the track. This deflexion form disappears with the distance on behalf of harmonic signal. Far from the source, the contribution of harmonic regime due to irregularities becomes more important.

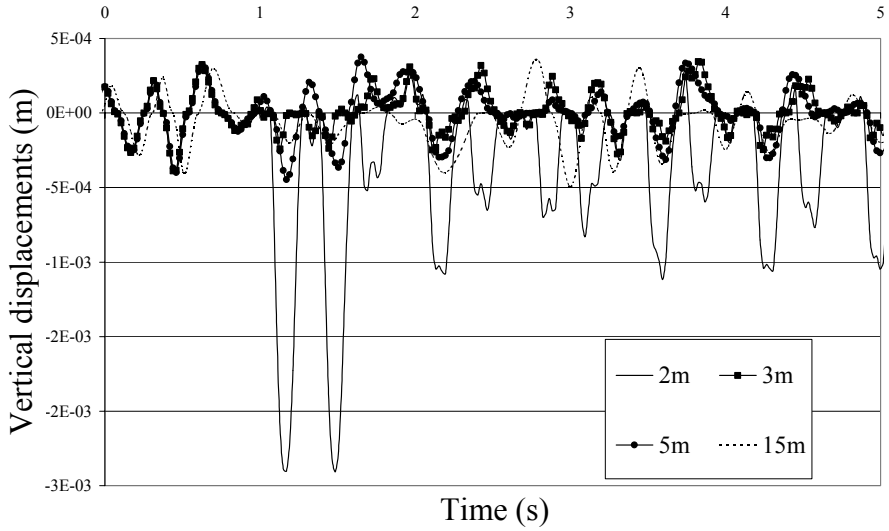


Figure 3 : Calculated responses at soil surface against distance from the track.

# 3 Comparison with *in-situ* measurements

## 3.1 Experimental results

Measurements were performed on 2 sites (See [2] for more details) in the North of France (Somme Bay) in the vicinity of a current railway track. In this area the soil is composed by peat and soft clay (very soft soil) lying on a limestone substratum (rock). Mechanical parameters and dynamical measurements were evaluated at the same time. The density of each different layer of *in-situ* soil was measured from a sound test. The Young modulus, Poisson's coefficient and damping ratio for each layer were performed from seismic measurements.

### 3.1.1 Description

To evaluate *in-situ* rails vibrations, an experimental device has been developed. In association with accelerometer and velocimeter, an optical technique is used for the local plane displacement measurement. Then the device allows to measure longitudinal and vertical displacements of the rail as well as deformations. Besides, it gives us an accurate value of the train speed thanks to an infrared detector

cutting the traffic way. As the camera is fixed in the vicinity of the track (2 metres), an accelerometer is laid on the ground near this latter in order to correct displacements transmitted from the ground to the optical system. An accelerometer is magnetized to the rail and can be used in a vertical or lateral position to confirm previous results. An other accelerometer is glued on a sleeper and allows to determine some information on pads behaviour. Finally five accelerometers are laid on the ground and the ballast. Distances between each of them can vary from a site to an other (function of estimated wavelengths and possibility of arrangement).

### 3.1.2 Equivalent model

Table 2 represents a simplified equivalent model for an *in-situ* soil. Compression (P) and shear (S) wave speeds are measured with a line of 24 sensors with 2 metres spacing and allow us to evaluate the layer depth , the damping $\eta$ (Barkan law [1]) and the mechanical parameters E et $\nu$. This equivalent model built according to Table 2 allows to supply the numerical model. The two studied sites are a bit different (different Young modulus and Poisson coefficient). Water contents are more or less important on these two sites. Then, in this paper, only one of the two sites will be introduced and build like in Table 2. The low Young modulus and the Poisson coefficient close to 0.5 can be noticed.

| | $C_p$ (m/s) | $C_s$ (m/s) | E (MPa) | $\nu$ | $\rho$ (kg/m$^3$) | $\eta$ |
|---|---|---|---|---|---|---|
| Peat (3m) | 345 | 122 | 68 | 0,43 | 1600 | 0.05 |
| Transition (4m) | 959 | 475 | 940 | 0,37 | 1850 | 0.08 |
| Limestone ($\infty$) | 1850 | 920 | 3889 | 0,35 | 2000 | 0.1 |

Table 2 : Mechanical parameters of *in-situ* site

### 3.1.3 Experimental results

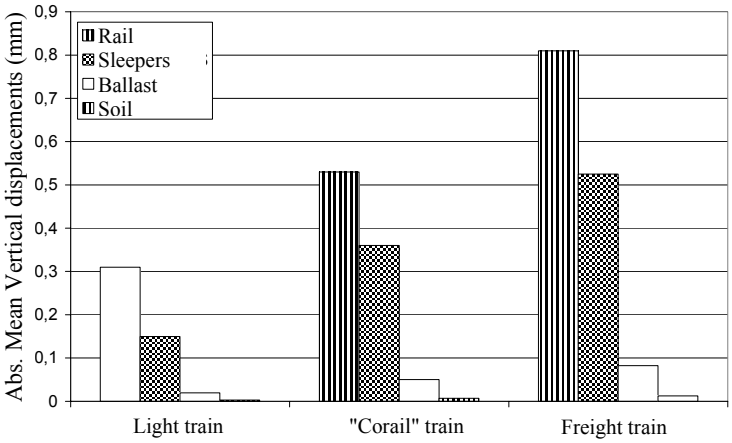


Figure 4 : State of vertical displacements measured on site.

A comparison between absolute averages of vertical displacements in each track element and for different types of traffic (Light, "Corail" and freight) with increase of weight load is plotted on Figure 4. This figure confirms previous results.

Attenuation between each element can be evaluated for three different types of trains and shows that behaviour at these relatively low speeds (70 and 140 km per hour) seems to be linear according to the weight.

## 3.2 Validation of the model

Figure 5 shows two comparisons between measurements obtained on site and numerical results deduced from FASTIVIB code. Excitation is composed by a constant part (non-harmonic) as well as a harmonic part (frequency from 5 to 80 Hz).

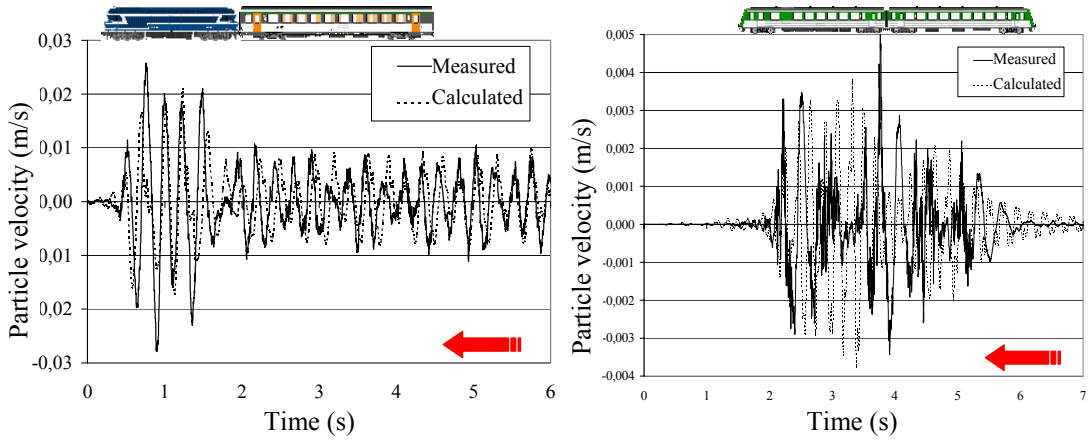


Figure 5 : Comparison between measurement and simulation.

Comparison between measurements and simulation results against distance from the track is also realised in Figure 6.

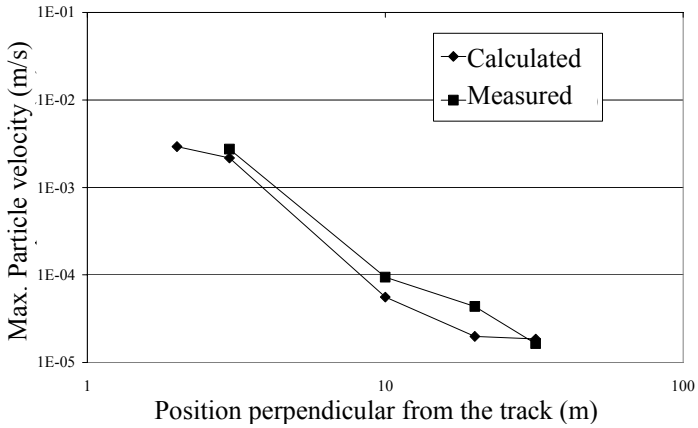


Figure 6 : Particle velocity of soil surface against the distance from track.

Numerical results were sometimes compared to experimental results for a single harmonic component in the range of resonance of the peat layer or more often for a large range of frequencies (function of wheel - rail excitation necessary to be evaluated for each frequency).

The good agreement found in Figure 6 between experimental and numerical results confirms the quality in the evaluation of mechanical parameters, especially those connected to P and S waves speeds and the damping law.

Finally, Figure 7 introduces a comparison between the measurements and simulation of displacements for a "Corail" train in terms of spectral density against the distance from the track. The farthest from the source the measurements were done, the more attenuated the higher frequency were found. This attenuation is more important in the range from 30 to 60 Hz up to five metres.

The spectral density of vertical displacements simulated with a multi - frequential model (from 0 to 80 Hz) (with a static component for moving masses and dynamic components representing wheel - rail interaction) is agreed with *in-situ* measurements.

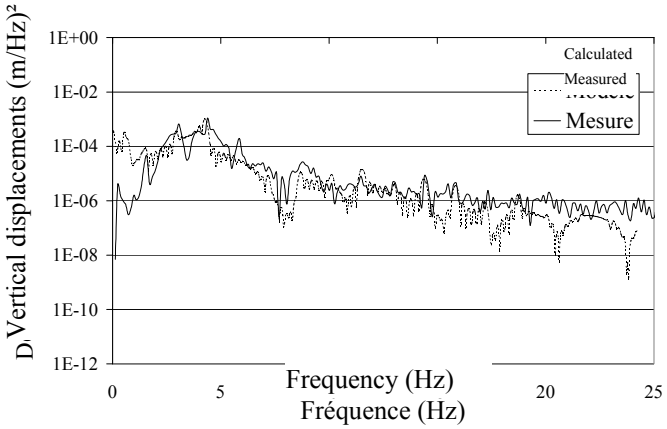


Figure 7 : Spectral density of vertical displacements
at 2 metres from the track for "Corail" train (135 km/h).

Other measurements at 2 or 5 metres in the case of different trains configuration (light, "Corail" or freight train) and for speeds from 70 to 140 km per hour were also compared. Except experimental problems due to sensitive equipment used in difficult conditions (humidity), results could be used to validate our numerical model in the range of frequency and for the parameters previously chosen.

Sometimes, displacements magnitudes are not exactly found with the model owing to the fact that several approximations have been done and evaluation of excitation frequency (single or multiple) of the load has been simplified. Last but not least, real effect of track element is probably not enough representative in the model (mainly ballast and pads certainly need non linear behaviours).

# 4 Conclusion

A three - dimensional model of railway track – layered soil interaction has been introduced. This model allows a fast study of the propagation of vibrations at the soil surface emitted by a railway train moving at constant speed. It includes the main linear parameters of train, track and layered soil. Besides, the validation of this model has been done thanks to several *in-situ* measurements on a very soft soil. Despite of difficulties due to in-situ measurements and uncertainties found in the two approaches (numerical and experimental), the comparison can be performed for particles velocities and displacements. The good agreement introduced in this paper is significant enough to estimate that the developed model is able to give suitable information on the behaviour of the track and the surrounding soil.

These studies allow the construction of an available data basis for future development of models. Besides, the set of these researches will permit to apprehend with a believable and suitable approach phenomena of wave propagation from vehicles (especially trains) moving at constant speed.

Afterwards, different numerical implementations will be performed in order to modify the soil or track parameters and then to imagine solutions for the reduction of this high vibrations. In this same object, a finite element model will be developed.

# References


[1] Degrande, C. , Lombaert, G., A dynamic soil structure interaction approach for the modeling of free field traffic induced vibrations, *7th International Congress on Sound and Vibration*, Garmisch-Partenkirchen (Germany), 4-7 July 2000, pp. 2671-2678

[2] Jones, D.V., Le Houédec, D., Peplow, A.T. & Petyt, M. 1998. Ground vibration in the vicinity of a moving harmonic rectangular load on a half space. *European Journal of Mechanics A/Solids* 17(1). pp. 153 – 166.

[3] Krylov, V.V. 1997. Spectra of low frequency ground vibrations generated by high speed trains on layered ground. *Journal of Low Frequency Noise Vibration and Active Control* 16(4). pp 257 - 270.

[4] Lefeuve-Mesgouez, G. 1999. Ground propagation due to load moving at constant speed. Ph D thesis (in French)*, Ecole Centrale of Nantes*. pp. 1 – 147.

[5] Madshus, C. & Kaynia, A.M. 2000. High speed railway lines on soft ground : dynamic behaviour at critical train speed. *Journal of Sound and Vibration* 231(3) : 689 - 701.

[6] Metrikine, A.V. & Popp, K. 1999. Vibration of a periodically supported beam on an elastic half space. *European Journal of Mechanics A/Solids* 18. pp. 679 - 701.

[7] Picoux, B. 2002. Theoretical and experimental researches on wave propagation in soil emitted by a railway traffic. Ph D thesis (in French)*, Ecole Centrale of Nantes*. pp. 1 – 155.

[8] Sheng, X., Jones, C.J.C. & Petyt, M. 1999. Ground vibration generated by a load moving along a railway track. *Journal of Sound and Vibration* 228(1). pp. 129 - 156.